Dibaryons and pentaquarks in quark models

Hongxia Huang (黄虹霞)
Nanjing Normal University

Collaborate with Jialun Ping and Fan Wang

强子物理新发展研讨会(网络会议)
2020.4.24-2020.4.26

Outline

I. Introduction

II. Dibaryon relevant studies

- Nonstrange dibaryon
- Strange dibaryon
- Dibaryon with heavy quarks

III. Pentaquark relevant studies

- Hidden-charm pentaquark
- Hidden-bottom pentaquark
- Hidden-strange pentaquark

VI. Summary

I. Introduction

Hadrons

- Quark model:

Mesons

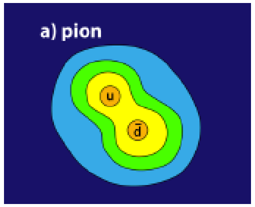

Baryons

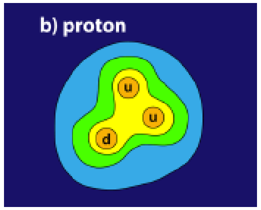

lowest configuration

- Exotic hadrons:

Glueball

Hybrid

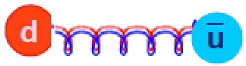

Molecule

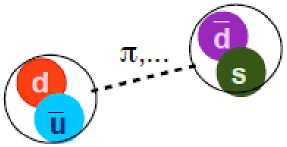

Clear **exotic signature:**

e.g. Exotic quantum numbers

Tetraquark

Pentaquark

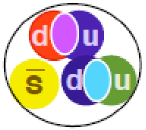

H-dibaryon

+ . . .

- **Exotic states**

Dibaryons: H, d^*, di-Ω, $N\Omega$, ……

Pentaquarks: Θ^+ , Ξ^{--} , P_c , Ωc , $N\phi$ ……

Charmonium-like states: X(3872), Y(3940), Z(3900), Z(4430),……

Plausible molecular baryons: $\Sigma_c D$, $\Lambda_c D$, DN, $D_s N$, ……

Dibaryons with heavy quarks: $\Lambda_c \Lambda_c$, $\Sigma_c \Sigma_c$, $\Xi_c \Xi_c$,

$N\Lambda_c$, $N\Sigma_c$, $N\Xi_{cc}$, $N\Omega_c$, ……

Exotic hadrons

—long standing challenge in hadron physics!

- **Theoretical methods**

  Lattice QCD

  QCD sum rule

  Dyson-Schwinger equation

  Heavy quark efficient field theory

  Phenomenological models of two approaches:

  On the hadron level:

  One-boson-exchange (OBE) model,

  One-pion-exchange (OPE) model

  ......

  On the quark level:

  Isgur quark model , Chiral quark model,

  Quark delocalization color screening model

  ......

- **Quark Models**

(1) Quark delocalization color screening model (QDCSM)

- QDCSM was developed by Nanjing-Los Alamos collaboration in1990s aimed to multi-quark study. (PRL 69, 2901, 1992)
- Two new ingredients (based on quark cluster model configuration):

  quark delocalization (orbital excitation)

  color screening (color structure)
- Apply to the study of baryon-baryon interaction and dibaryons

  deuteron, d, NN, NΛ, NΩ, …*
- Apply to the study of baryon-meson interaction and pentaquarks

  NK, Npi, Pc, …

$$
\begin{aligned}
H &= \sum_{i=1}^{6}\left(m_i + \frac{p_i^2}{2m_i}\right) - T_c + \sum_{i<j}[V^G(r_{ij}) + V^\chi(r_{ij}) + V^C(r_{ij})],\\
V^G(r_{ij}) &= \frac{1}{4}\alpha_s \lambda_i \cdot \lambda_j \left[\frac{1}{r_{ij}} - \frac{\pi}{2}\left(\frac{1}{m_i^2} + \frac{1}{m_j^2} + \frac{4\sigma_i \cdot \sigma_j}{3m_i m_j}\right)\delta(r_{ij}) - \frac{3}{4m_i m_j r_{ij}^3} S_{ij}\right],\\
V^\chi(r_{ij}) &= \frac{1}{3}\alpha_{ch}\frac{\Lambda^2}{\Lambda^2 - m_\chi^2} m_\chi \left\{\left[Y(m_\chi r_{ij}) - \frac{\Lambda^3}{m_\chi^3} Y(\Lambda r_{ij})\right]\sigma_i \cdot \sigma_j + \left[H(m_\chi r_{ij}) - \frac{\Lambda^3}{m_\chi^3} H(\Lambda r_{ij})\right] S_{ij}\right\} \mathbf{F}_i \cdot \mathbf{F}_j,\ \chi = \pi, K, \eta,\\
V^C(r_{ij}) &= -a_c \lambda_i \cdot \lambda_j [f(r_{ij}) + V_0],\\
f(r_{ij}) &= \begin{cases} r_{ij}^2 & \text{if } i, j \text{ occur in the same baryon orbit,} \\ \frac{1 - e^{-\mu_{ij} r_{ij}^2}}{\mu_{ij}} & \text{if } i, j \text{ occur in different baryon orbits,} \end{cases}\\
S_{ij} &= \frac{(\sigma_i \cdot \mathbf{r}_{ij})(\sigma_j \cdot \mathbf{r}_{ij})}{r_{ij}^2} - \frac{1}{3}\sigma_i \cdot \sigma_j, \qquad (1)
\end{aligned}
$$

(2) Chrial Quark Model (ChQM)

Provide the intermediate-range attraction by σ meson-exchange.

Rep. Prog. Phys. 68, 965 (2005)

SU(2) ChQM: only σ meson-exchange;

$$V_{ij}^{\sigma} = -\frac{g_{ch}^2}{4\pi}\frac{\Lambda_\sigma^2}{\Lambda_\sigma^2 - m_\sigma^2} m_\sigma \left[Y(m_\sigma r_{ij}) - \frac{\Lambda_\sigma}{m_\sigma} Y(\Lambda_\sigma r_{ij}) \right]$$

SU(3) ChQM: full scalar octet meson-exchange.

PRC 75, 034002 (2007)

$$V_{ij}^{\sigma_a} = V_{a_0}(r_{ij}) \sum_{a=1}^{3} \lambda_i^a \cdot \lambda_j^a + V_\kappa(r_{ij}) \sum_{a=4}^{7} \lambda_i^a \cdot \lambda_j^a + V_{f_0}(r_{ij}) \lambda_i^8 \cdot \lambda_j^8 + V_\sigma(r_{ij}) \lambda_i^0 \cdot \lambda_j^0$$

II. Dibaryon relevant studies

1. Nonstrange dibaryon (d*)

➢ WASA-at-COSY measurements

- 2009 WASA-at-COSY found the signal of the dibaryon resonance.

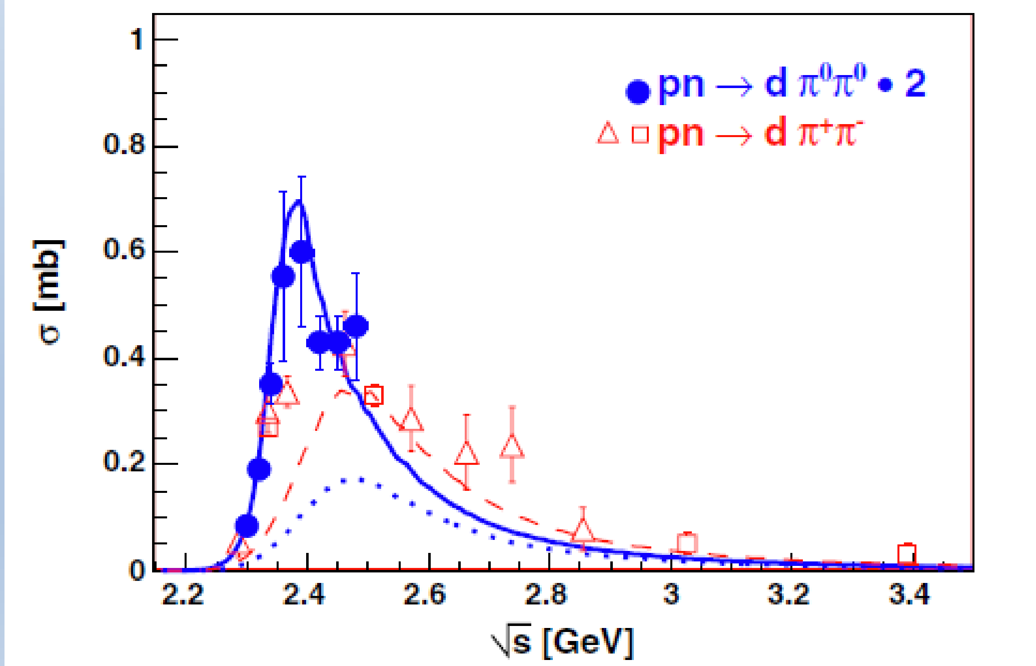

M. Bashkanov et al., PRL 102(2009)052301

- 2011 WASA-at-COSY found evidence of the d* exotic.

M. Bashkanov et al., arxiv:1104.0123[nucl-ex];

PRL 106(2011)242302;

.

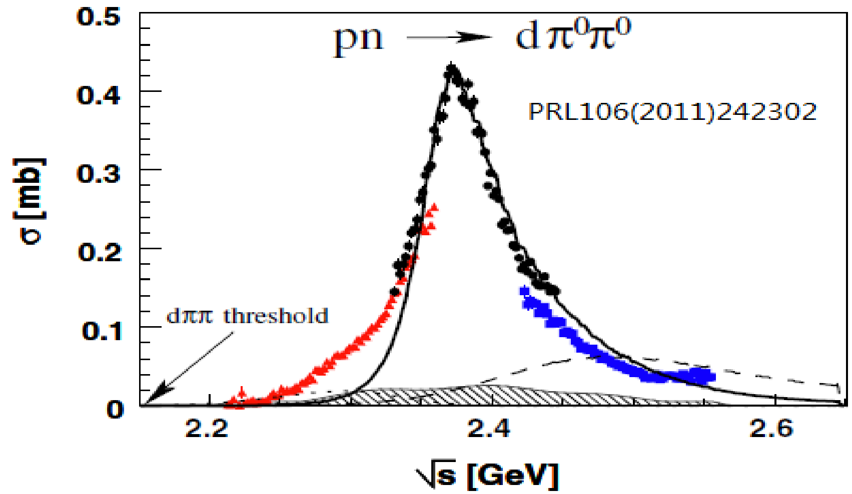

FIG. 2 (color online). Total cross sections obtained from this experiment on $pd \to d\pi^0\pi^0 + p_{\rm spectator}$ for the beam energies $T_p = 1.0$ GeV (triangles), 1.2 GeV (dots), and 1.4 GeV (squares) normalized independently. Shown are the total cross section data after acceptance, efficiency and Fermi motion corrections. The hatched area indicates systematic uncertainties. The drawn lines represent the expected cross sections for the Roper excitation process (dotted) and the t-channel $\Delta\Delta$ contribution (dashed) as well as a calculation for a s-channel resonance with $m = 2.37$ GeV and $\Gamma = 68$ MeV (solid).

$$\boxed{m = 2.37\ \text{GeV}, \Gamma \approx 70\ \text{MeV and } I(J^P) = 0(3^+)}$$

- 2014 WASA-at-COSY confirmed the existence of the d* six-quark state.

P. Adlarson et al, arXiv:1402.6844[nucl-es];PRL 112(2014)202301;

CERN Courier 2014, July 23.

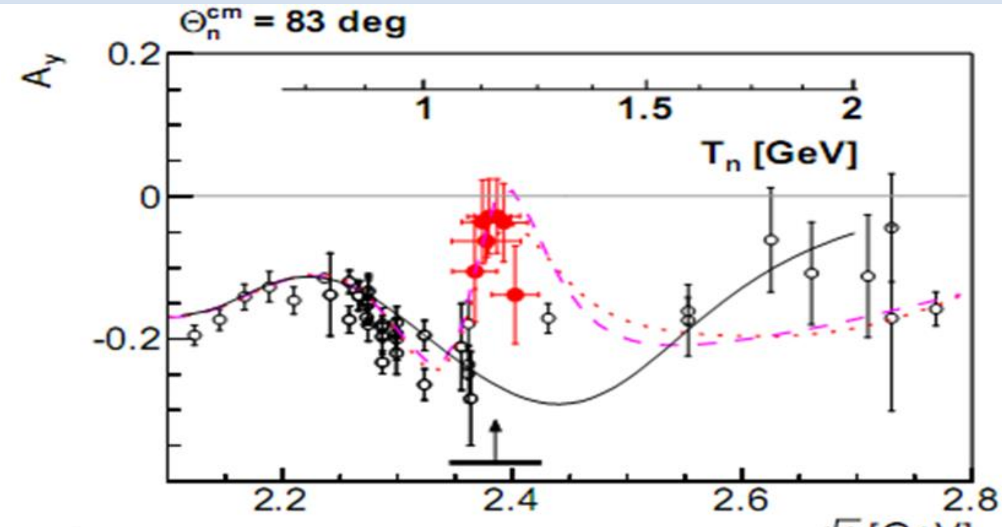

arXiv:1402.6844 PRL 112 (2014) 202301

FIG. 4: (Color online) Energy dependence of the np analyzing power at $\Theta_n^{cm} = 83°$. The solid symbols denote the results from this work, the open symbols those from previous work [7–9, 21–25]. For the meaning of the curves see Fig. 1. Vertical arrow and horizontal bar indicate pole and width of the resonance.

The experiment was carried out with the WASA detector setup at COSY having a polarized deuteron beam impinged on the hydrogen pellet target and utilizing the quasifree process

$$\vec{d}p \rightarrow np + p_{\rm spectator}$$

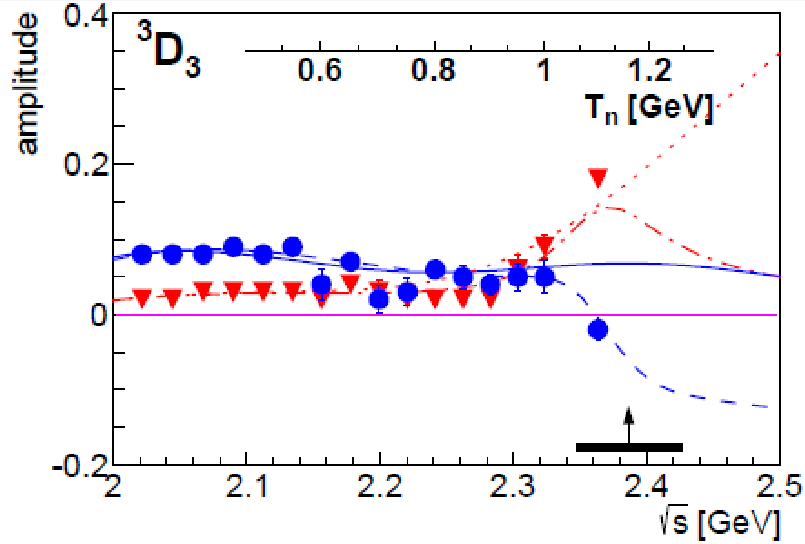

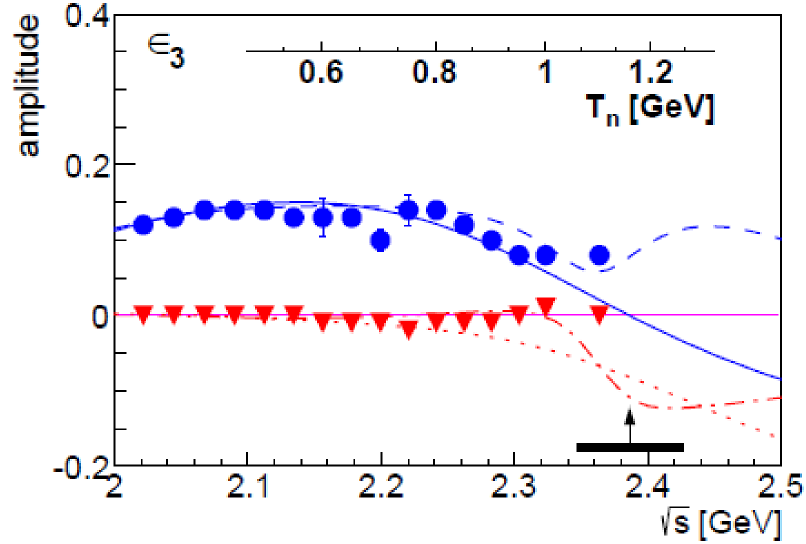

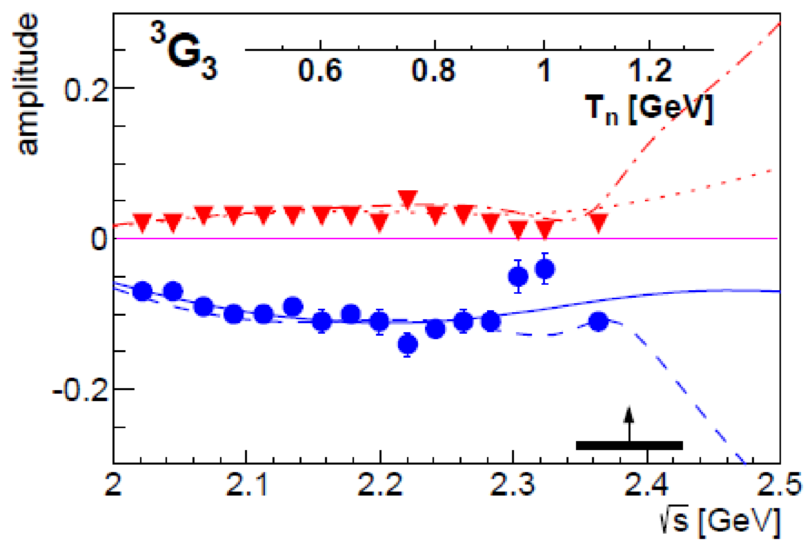

FIG. 3: (Color online) Changes to the (dimensionless) $^3D_3$ (top) and $^3G_3$ (middle) partial waves including their mixing amplitude ϵ_3 (bottom). Solid (dotted) curves give the real (imaginary) part of the partial-wave amplitudes from SP07, whereas the dashed (dash-dotted) curves represent the new (weighted) solution. Results from previous single energy fits [16] are shown by solid circles (real part) and inverted triangles (imaginary part). Vertical arrow and horizontal bar indicate pole and width of the resonance.

A2 Collaboration at MAMI

M. Bashkanov et al.,
PRL 124, 132001 (2020)

Signatures of the $d^*(2380)$ Hexaquark in $d(\gamma,p\vec{n})$

(A2 Collaboration at MAMI)

We report a measurement of the spin polarization of the recoiling neutron in deuterium photodisintegration, utilizing a new large acceptance polarimeter within the Crystal Ball at MAMI. The measured photon energy range of 300–700 MeV provides the first measurement of recoil neutron polarization at photon energies where the quark substructure of the deuteron plays a role, thereby providing important new constraints on photodisintegration mechanisms. A very high neutron polarization in a narrow structure centered around $E_\gamma \sim 570$ MeV is observed, which is inconsistent with current theoretical predictions employing nucleon resonance degrees of freedom. A Legendre polynomial decomposition suggests this behavior could be related to the excitation of the $d^*(2380)$ hexaquark.

➢ Theoretical side

- 1964, Dyson & Xuong, M(D_{03})=2350 MeV (PRL13, 815)

  naïve quark model prediction almost forgotten in last 50 years
- 1989, T. Goldman,…,Fan Wang, (PRC 39, 1889)

  "inevitable nonstrange dibaryon" d*
- 1992, Fan Wang, et al., (PRL 69, 2901) confirmed by QDCSM
- 1995, Fan Wang, JL Ping, et al, (PRC 51, 3411)

  further confirmed by u,d,s 3-flavor world systematic searching
- 2002, JL Ping, Fan Wang, et al., (PRC 65, 044003) improved d* calculation
- 2009, JL Ping et al, (PRC 79, 024001) d* in np resonance scattering
- 2013, Bashkanov, S. Brodsky, H. Clement, (PLB 727, 438)

  hidden-color → narrow width
- 2013, A.Gal, H. Garcilaso, (PRL 111, 12301) Faddeev equation
- 2014, F. Huang et al, arXiv:1408.0458 hidden-color → narrow width
- 2015, Y.B. Dong, (PRC 91, 064002) d* decay width
- 2015, S.L. Zhu, et al.,(PRC 91, 025204) QCD sum rule

……

➢ d* in quark models

(1) d* mass and width in NN- $\Delta\Delta$ channel coupling scattering

PRC 79 (2009) 024001

N_{ch}	ChQM2		ChQM2a		QDCSM0		QDCSM1		QDCSM3	
	M	Γ	M	Γ	M	Γ	M	Γ	M	Γ
1c	2425	–	2430	–	2413	–	2365	–	2276	–
2cc	2428	17	2433	10	2416	20	2368	20	2278	19
4cc	2413	14	2424	9	2400	14	$\boxed{2357}$	$\boxed{14}$	2273	17
10cc	2393	14			–	–	–	–	–	–
10cc′	2353	17			–	–	–	–	–	–
10cc″	2351	21			–	–	–	–	–	–

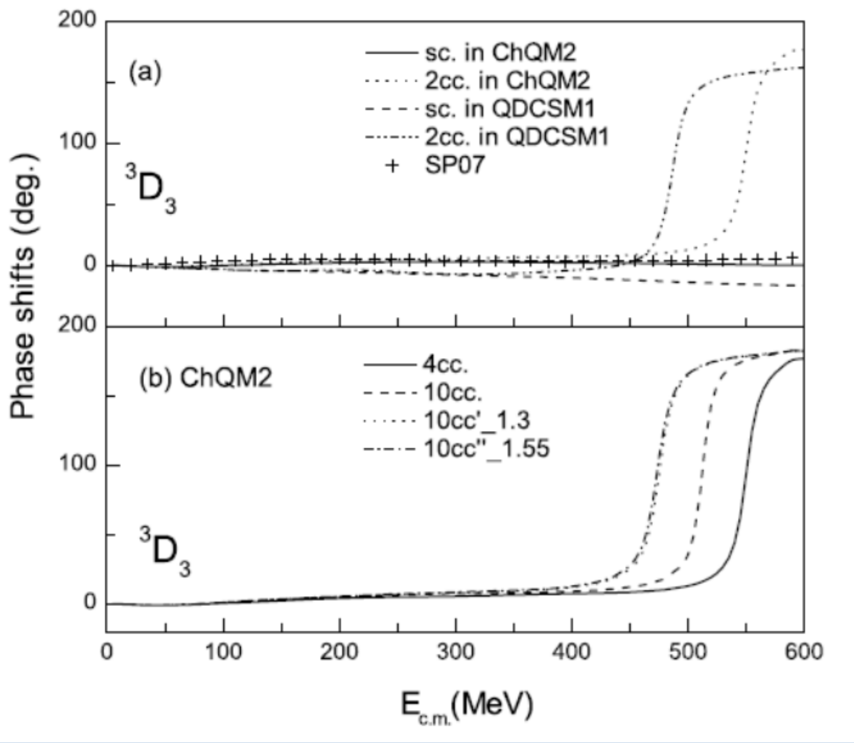

(2) Total decay width of d*

ChQM2:	
M_R	2393
Γ_{NN}	14
Γ_{inel}	136
B_{NN}	0.09

QDCSM1:	
M_R	2357
Γ_{NN}	14
Γ_{inel}	96
B_{NN}	0.13

Only phase space reduction:

(structure of d* is not considered)

$$\Gamma_{b\Delta}(M_{b\Delta}) \approx \Gamma_{f\Delta}\frac{k_b^{2\ell}\rho(M_{b\Delta})}{k_f^{2\ell}\rho(M_{f\Delta})},$$

[33] B. Julia-Diaz, T.-S. H. Lee, A. Matsuyama, and T. Sato, Phys. Rev. C **76**, 065201 (2007).

The rms radius is about 1fm.
d* is a compact six quark state, two baryon clustering is a crude approximation.

(3) d* in the D-G partial waves of NN scattering

PRC 90 (2014) 064003

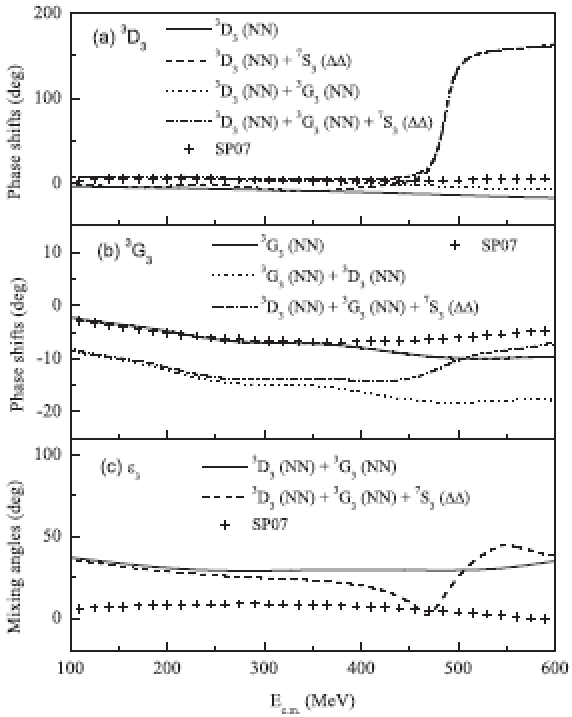

FIG. 1. $^3D_3^{NN}$ and $^3G_3^{NN}$ phase shifts including their mixing angles ε_3 in QDCSM.

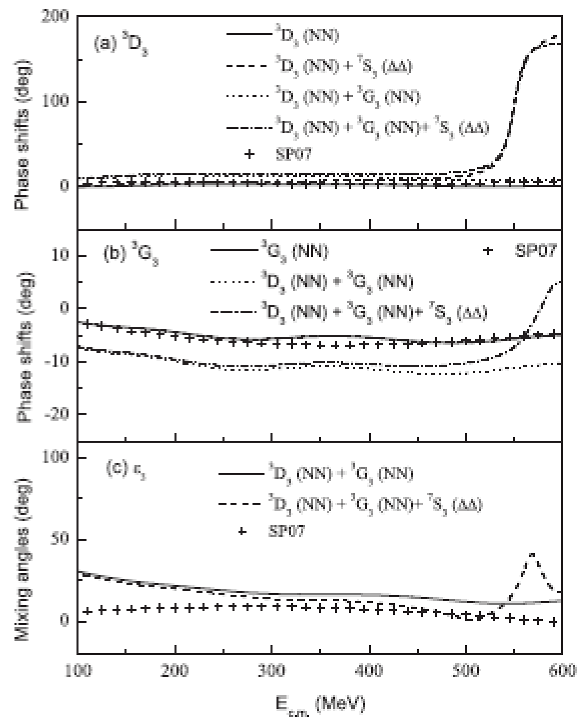

FIG. 2. $^3D_3^{NN}$ and $^3G_3^{NN}$ phase shifts including their mixing angles ε_3 in ChQM.

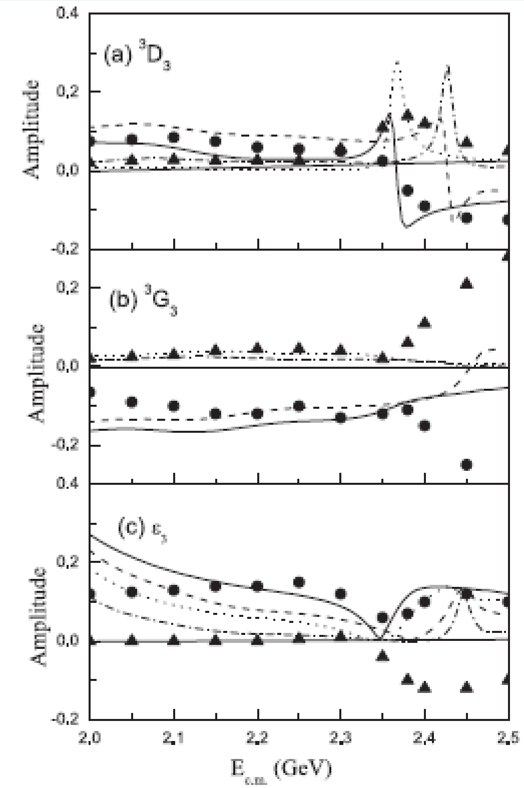

FIG. 3. $^3D_3^{NN}$ and $^3G_3^{NN}$ amplitudes including their mixing amplitude ε_3 in two quark models. Solid (dotted) curves give the real (imaginary) part of partial-wave amplitudes in QDCSM, whereas the dashed (dash-dotted) curves represent the real (imaginary) part of partial-wave amplitudes in ChQM. Results from Ref. [6] are shown as solid circles (real part) and solid triangles (imaginary part).

2. Strange dibaryon (NΩ)

- Might be a narrow **resonance**. PRL 59,627 (1987)
- A very narrow **resonance**.
- PRC 51, 3411 (1995); PRC 69,065207 (2004)
- A weakly **bound** state. EPJA 8, 417 (2000)
- A narrow **resonance** in $\Lambda\Xi$ scattering. PRC 83, 015202 (2011)
- Further theoretical work to confirm the NΩ. PRC 92, 065202 (2015)

(NΩ scattering phase shifts, the scattering length and the effective range)

HALQCD Collaboration, Nucl. Phys. A 928, 89 (2014)

Being searched by RHIC-STAR Collaboration, Phys.Lett. B 790, 490 (2019).

Systematically searching for strange dibaryon states

PRC 83,015202 (2011)

S	I	J	State	M(MeV)	Γ(MeV)	Decay channels
-1	$\frac{1}{2}$	3	$\Delta\Sigma^*$	2440-2540	48-118	$N\Lambda$ or $N\Sigma$
-2	0	2	$N\Xi^*$	2400-2430	10-11	$N\Xi$ or $\Lambda\Lambda$
-2	1	3	$\Delta\Xi^*$	2620-2660	50-90	$N\Xi$
-3	$\frac{1}{2}$	2	$N\Omega$	2528-2547	2-4	$\Lambda\Xi$
-3	$\frac{3}{2}$	3	$\Sigma^*\Xi^*$	2788-2795	50-60	$\Sigma\Xi$

➢ The NΩ scattering phase shifts

PRC 92,065202 (2015)

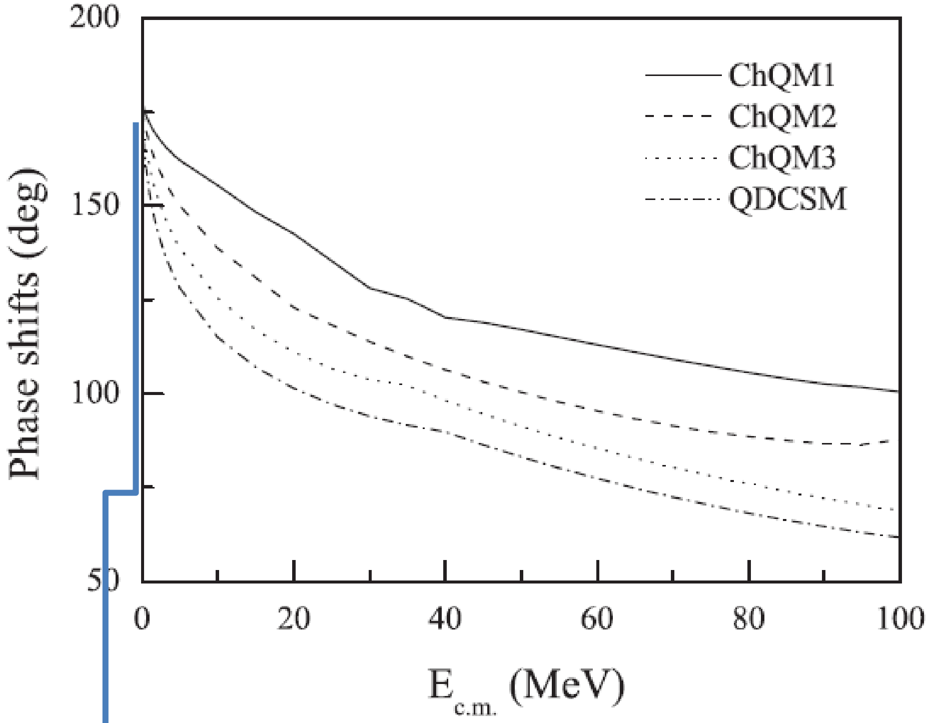

FIG. 2. The phase shifts of S-wave $N\Omega$ dibaryon.

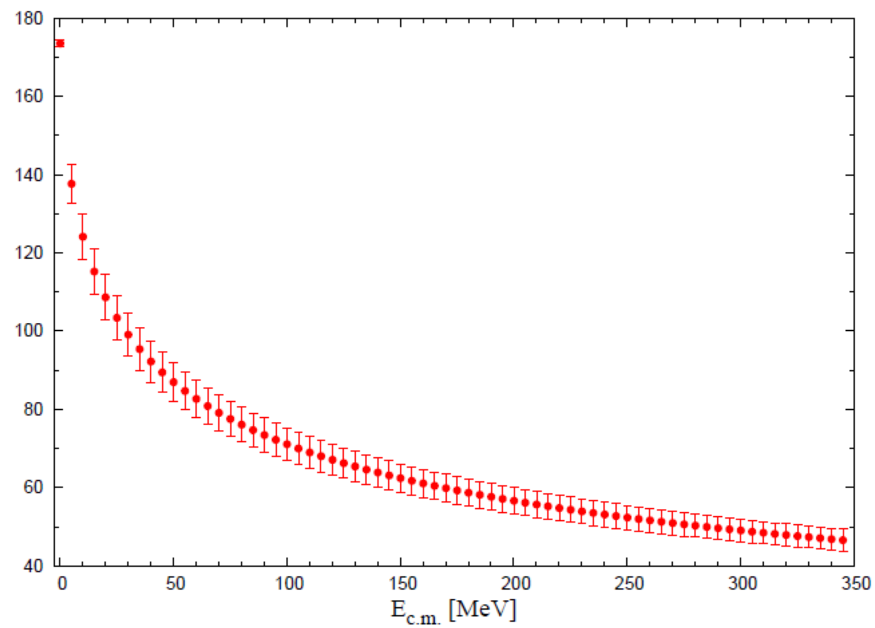

HALQCD Collaboration
Nucl. Phys. A 928, 89 (2014)

implies the existence of a bound state

➢ The scattering length, the effective range and the binding energy

$$k\cot\delta = -\frac{1}{a_0} + \frac{1}{2}r_0k^2 + \mathcal{O}(k^4)$$

$$B = \frac{\hbar^2\alpha^2}{2\mu} \qquad r_0 = \frac{2}{\alpha}(1 - \frac{1}{\alpha a_0})$$

TABLE VI. The scattering length a_0, effective range r_0, and binding energy B' of the $N\Omega$ dibaryon.

	a_0 (fm)	r_0 (fm)	B' (MeV)
QDCSM	2.8007	0.5770	–5.2
ChQM1	0.8103	0.3609	–110.3
ChQM2	1.3808	0.6018	–37.3
ChQM3	1.9870	0.7064	–13.7

$$B_{N\Omega} = 18.9(5.0)(^{+12.1}_{-1.8})\ \mathrm{MeV},$$
$$a_{N\Omega} = -1.28(0.13)(^{+0.14}_{-0.15})\ \mathrm{fm},$$
$$(r_e)_{N\Omega} = 0.499(0.026)(^{+0.029}_{-0.048})\ \mathrm{fm}.$$

HALQCD Collaboration
Nucl. Phys. A 928, 89 (2014)

Physics Letters B 790 (2019) 490–497

Contents lists available at ScienceDirect

Physics Letters B

www.elsevier.com/locate/physletb

The proton–Ω correlation function in Au + Au collisions at $\sqrt{s_{NN}} = 200$ GeV

STAR Collaboration

ABSTRACT

We present the first measurement of the proton–Ω correlation function in heavy-ion collisions for the central (0–40%) and peripheral (40–80%) Au + Au collisions at $\sqrt{s_{NN}} = 200$ GeV by the STAR experiment at the Relativistic Heavy-Ion Collider (RHIC). Predictions for the ratio of peripheral collisions to central collisions for the proton–Ω correlation function are sensitive to the presence of a nucleon–Ω bound state. These predictions are based on the proton–Ω interaction extracted from $(2+1)$-flavor lattice QCD calculations at the physical point. The measured ratio of the proton–Ω correlation function between the peripheral (small system) and central (large system) collisions is less than unity for relative momentum smaller than 40 MeV/c. Comparison of our measured correlation ratio with theoretical calculation slightly favors a proton–Ω bound system with a binding energy of ~ 27 MeV.

3. Dibaryon with heavy quarks

(1) H-like dibaryon states: $\Lambda c \Lambda c$, Λb Λb

PRC 89 ,035201,2014

Is the H dibaryon $\Lambda\Lambda$ a bound state?

First proposed by R. L. Jaffe

PRL 38, 195, 1977

Revived by Lattice QCD calculations of different collaborations:

NPLQCD, PRL 106, 162001, 2011

HALQCD, PRL 106, 162002, 2011

Reexamined in a chiral constituent quark model

PRC 85, 045202, 2012

Is the H-like dibaryon $\Lambda c \Lambda c$ a bound state?

Answers of two hadron level models

No in One-boson-exchange model PRD 84, 014031, 2011

Yes in One-pion-exchange model PLB 704, 547, 2011

What about the quark level study of the $\Lambda c \Lambda c$ system?

$^{2S+1}L_J$

TABLE III. The $\Lambda_c\Lambda_c$ and $\Lambda_b\Lambda_b$ states and the channels coupled to them.

Channels	1	2	3	4	5	6	7
$J^P=0^+$	$\Sigma_c\Sigma_c(^1S_0)$	$N\Xi_{cc}(^1S_0)$	$\Lambda_c\Lambda_c(^1S_0)$	$\Sigma_c^*\Sigma_c^*(^1S_0)$	$N\Xi_{cc}^*(^5D_0)$	$\Sigma_c\Sigma_c^*(^5D_0)$	$\Sigma_c^*\Sigma_c^*(^5D_0)$
$J^P=0^+$	$\Sigma_b\Sigma_b(^1S_0)$	$N\Xi_{bb}(^1S_0)$	$\Lambda_b\Lambda_b(^1S_0)$	$\Sigma_b^*\Sigma_b^*(^1S_0)$	$N\Xi_{bb}^*(^5D_0)$	$\Sigma_b\Sigma_b^*(^5D_0)$	$\Sigma_b^*\Sigma_b^*(^5D_0)$

- The individual S-wave $\Lambda_c\Lambda_c$ is unbound. A bound state is obtained for the $\Lambda_c\Lambda_c$ system by channel-coupling.

TABLE IV. The binding energy B.E. (MeV) of every $^1S_0$ channel of the $\Lambda_c\Lambda_c$ system, and channel coupling (c.c.).

Channels	$\Sigma_c\Sigma_c$	$N\Xi_{cc}$	$\Lambda_c\Lambda_c$	$\Sigma_c^*\Sigma_c^*$	c.c.
QDCSM1	−35.4	ub	ub	−30.4	−3.3
QDCSM2	−75.4	ub	ub	−87.0	−19.4

➢Similar to H dibaryon: $\Lambda\Lambda$ system (PRC 69, 065207,2004)

S,I,J	Coupling channels	Mass$_{sc}$	Mass$_{cc}$
$-2,0,0$	$\Lambda\Lambda$-$N\Xi-\Sigma\Sigma$	-	2225.5

The single channel $\Lambda\Lambda$ is unbound, but when coupled to the channels $N\Xi$ and $\Sigma\Sigma$, it becomes a weakly bound state.
It is possible to form a bound state in the $\Lambda_c\Lambda_c$ system, with a binding energy of $3.0 \sim 20$ MeV, which is a H-like dibaryon state.

➢ $\Lambda_b\Lambda_b$ system

TABLE V. The binding energy B.E. (MeV) of every $^1S_0$ channel of the $\Lambda_b\Lambda_b$ system, and channel coupling (c.c.).

Channels	$\Sigma_b\Sigma_b$	$N\Xi_{bb}$	$\Lambda_b\Lambda_b$	$\Sigma_b^*\Sigma_b^*$	c.c
QDCSM1	−36.0	ub	ub	−28.2	−3.6
QDCSM2	−78.8	ub	ub	−83.0	−19.7

The results are similar to the $\Lambda_c\Lambda_c$ system. There is also an H-like dibaryon state in the $\Lambda_b\Lambda_b$ system with a binding energy of $3.0 \sim 20$ MeV in our quark model.

(2) NΩ-like dibaryons with heavy quarks: $N\Omega_{ccc}$, $N\Omega_{bbb}$

$IJ^P = \frac{1}{2}2^+$

PRC 101, 015204, 2020

TABLE III. Channels of the $N\Omega_{ccc}$ system.

1	2	3	4	5	6	7	8
$\Xi^*_{cc}\Sigma_c$	$\Xi_{cc}\Sigma^*_c$	$\Xi^*_{cc}\Lambda_c$	$N\Omega_{ccc}$	$\Xi^*_{cc}\Sigma^*_c$	$\Xi''_{cc}\Sigma^{*\prime}_c$	$\Xi^{*\prime}_{cc}\Sigma''_c$	$\Xi''_{cc}\Sigma''_c$
9	10	11	12	13	14	15	16
$\Xi''\Sigma$	$N'\Omega'_{ccc}$	$\Xi^{*\prime}_{cc}\Lambda''_c$	$\Xi'_{cc}\Lambda''_c$	$\Xi''_{cc}\Lambda''_c$	$\Xi''_{cc}\Lambda'''_c$	$\Xi'_{cc}\Sigma''_c$	$\Xi''_{cc}\Lambda'_c$

TABLE IV. The binding energies of the $N\Omega_{ccc}$ system with channel coupling.

	B_{sc} (MeV)	B_{5cc} (MeV)	B_{16cc} (MeV)
ChQM	ub	ub	−16.4
QDCSM	−0.6	−30.9	···

TABLE VI. The binding energies of the $N\Omega_{bbb}$ system with channel coupling.

	B_{sc} (MeV)	B_{5cc} (MeV)	B_{16cc} (MeV)
ChQM	ub	ub	−16.4
QDCSM	ub	−50.7	—

- Both of these two states are bound in two quark models: ChQM and QDCSM.
- The binding energy increases as the quark of the system becomes heavier.
- The effect of the channel-coupling is important for forming bound states.

➢ The scattering phase shifts, scattering length, the effective range and the binding energy

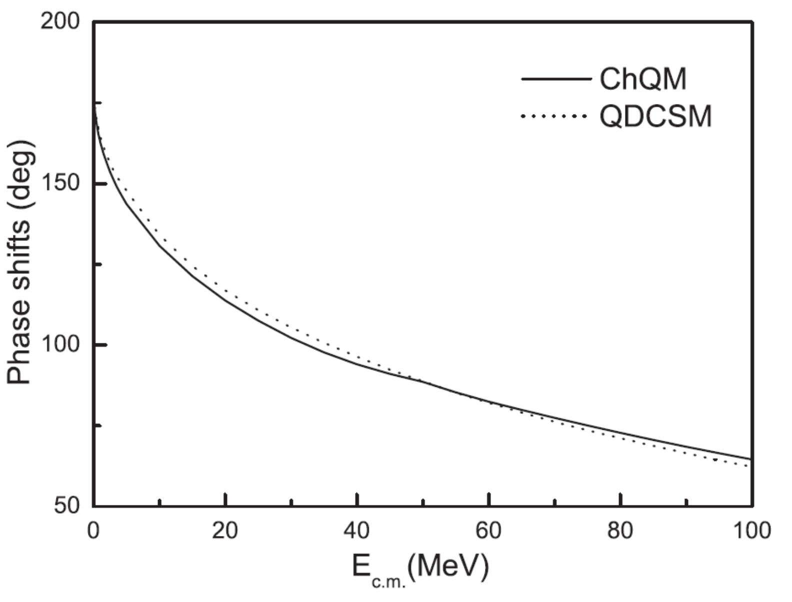

FIG. 2. The phase shifts of the $N\Omega_{ccc}$ state in both the ChQM and QDCSM.

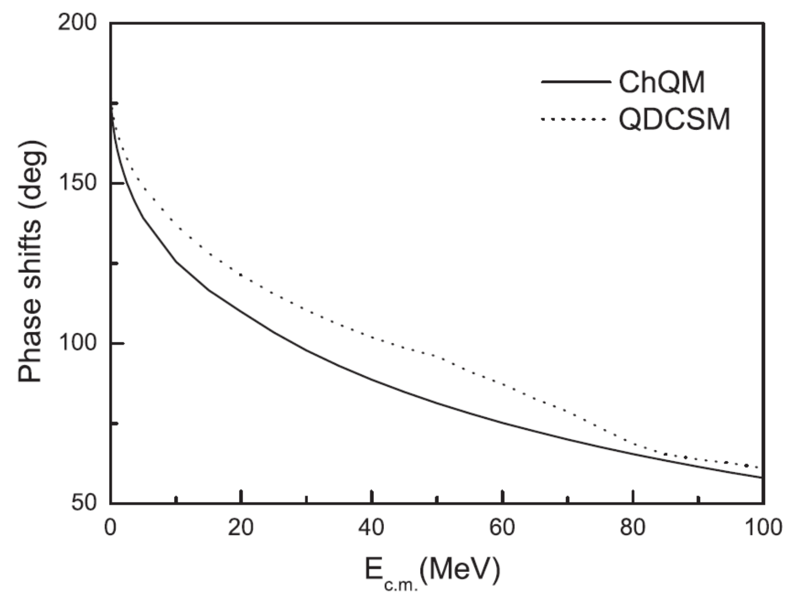

FIG. 3. The phase shifts of the $N\Omega_{bbb}$ state in both the ChQM and QDCSM.

TABLE V. The scattering length a_0, effective range r_0, and binding energy B' of the $N\Omega_{ccc}$ state.

	a_0 (fm)	r_0 (fm)	B' (MeV)
ChQM	1.4989	0.40810	−15.5
QDCSM	1.3347	0.43343	−21.6

TABLE VII. The scattering length a_0, effective range r_0, and binding energy B' of the $N\Omega_{bbb}$ state.

	a_0 (fm)	r_0 (fm)	B' (MeV)
ChQM	1.5981	0.66427	−40.1
QDCSM	1.1608	0.53617	−40.1

III. Pentaquark relevant studies

➢ Experimental results

- **2015** LHCb Collaboration, Phys. Rev. Lett. 115, 072001

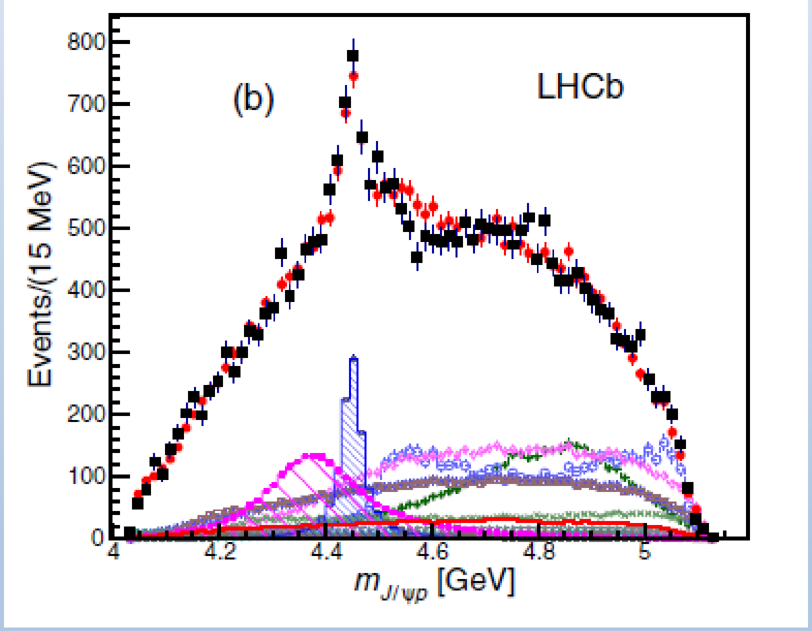

- The two P_c^+ states are found to have **masses and widths** of
  $M_{P_c\,(4380)} = 4380 \pm 8 \pm 29$ MeV
  $\Gamma_{P_c\,(4380)} = 205 \pm 18 \pm 86$MeV
  $M_{P_c\,(4450)} = 4449.8 \pm 1.7 \pm 2.5$ MeV
  $\Gamma_{P_c\,(4450)} = 39 \pm 5 \pm 19$ MeV

- The preferred **spin-parity J^P** are of opposite values, with one state having spin 3/2 and the other 5/2.

- **2019** LHCb Collaboration, Phys. Rev. Lett. 122 222001

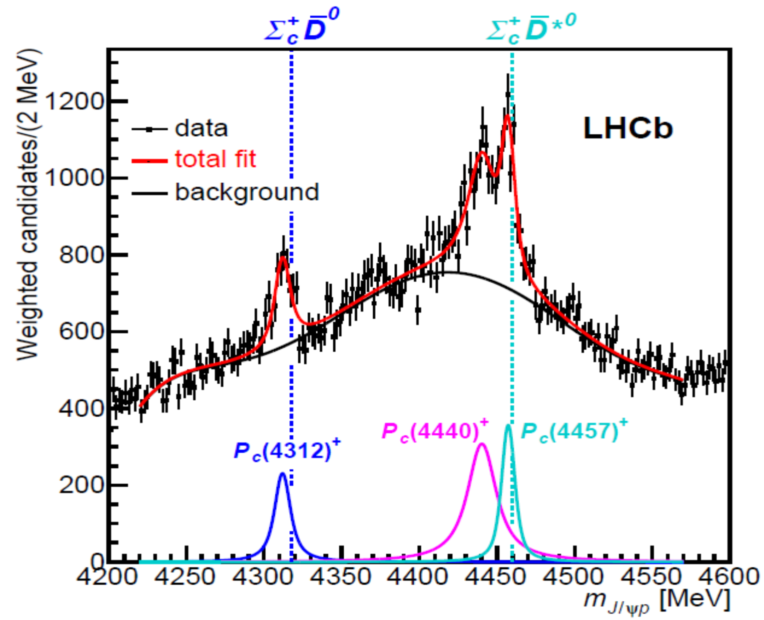

Figure 6: Fit to the $\cos\theta_{P_c}$-weighted $m_{J/\psi p}$ distribution with three BW amplitudes and a sixth-order polynomial background. This fit is used to determine the central values of the masses and widths of the P_c^+ states. The mass thresholds for the $\Sigma_c^+ \bar{D}^0$ and $\Sigma_c^+ \bar{D}^{*0}$ final states are superimposed.

- The *Pc*(4312) was discovered with 7.3*σ* significance by analyzing the *J/ψp* invariant mass spectrum.
- The previously reported *Pc*(4450) structure was resolved at 5.4*σ* significance into two narrow states: the *Pc*(4440) and *Pc*(4457).

Table 1: Summary of P_c^+ properties. The central values are based on the fit displayed in Fig. 6.

State	M [MeV]	Γ [MeV]	(95% CL)	$\mathcal{R}$ [%]
$P_c(4312)^+$	$4311.9 \pm 0.7^{+6.8}_{-0.6}$	$9.8 \pm 2.7^{+\ 3.7}_{-\ 4.5}$	(< 27)	$0.30 \pm 0.07^{+0.34}_{-0.09}$
$P_c(4440)^+$	$4440.3 \pm 1.3^{+4.1}_{-4.7}$	$20.6 \pm 4.9^{+\ 8.7}_{-10.1}$	(< 49)	$1.11 \pm 0.33^{+0.22}_{-0.10}$
$P_c(4457)^+$	$4457.3 \pm 0.6^{+4.1}_{-1.7}$	$6.4 \pm 2.0^{+\ 5.7}_{-\ 1.9}$	(< 20)	$0.53 \pm 0.16^{+0.15}_{-0.13}$

➢ Theoretical studies

- After LHCb’s Pc results (2015)

1) Loosely bound molecular baryon-meson pentaquark states:

M. Karliner and J. L. Rosner, Phys. Rev. Lett. 115, 122001 (2015).

R. Chen, X. Liu, X.-Q. Li, S.-L. Zhu, Phys.Rev.Lett. 115, no.13, 132002 (2015).

H. X. Chen, W. Chen, X. Liu, T.G. Steele and S. L. Zhu, Phys.Rev.Lett. 115, no.17, 172001 (2015) .

L. Roca, J. Nieves and E. Oset, Phys. Rev. D 92, 094003 (2015).

J. He, Phys.Lett. B753, 547-551 (2016) .

H. X. Huang, C. R. Deng, J. L. Ping, and F. Wang, Eur. Phys. J. C 76, 624 (2016).

H. X. Huang and J. L. Ping, Phys. Rev. D 99, 014010 (2019).

G. Yang and J. L. Ping, Phys. Rev. D 95, 010014 (2017).

A. Feijoo, V. K. Magas, A. Ramos and E. Oset, Phys. Rev. D 95, no.3, 039905 (2017).

and others.

2) Tightly bound pentaquark states

L. Maiani, A.D. Polosa, and V. Riquer, Phys.Lett. B 749, 289-291 (2015).

R. F. Lebed, Phys.Lett. B 749, 454-457 (2015).

G.-N. Li, X.-G. He, M. He, JHEP 1512, 128 (2015).

Z.-G. Wang, Eur. Phys. J. C 76, no.2, 70 (2016).

R. Zhu and C. F. Qiao, Phys.Lett. B 756, 259 (2016).
V. V. Anisovich et al., arXiv:1507.07652.
R. Ghosh, A. Bhattacharya, and B. Chakrabarti, Phys. Part. Nucl. Lett. 14, 550 (2017).

and others.

3) Peaks due to triangle-diagram processes

F.-K. Guo, U.-G. Meißner, W. Wang, and Z. Yang, Phys. Rev. D 92, 071502(R) (2015).
U.-G. Meißner and J. A. Oller, Phys. Lett. B 751, 59 (2015).
X.-H. Liu, Q. Wang, and Q. Zhao, Phys. Lett. B 757, 231 (2016).
Q. Wang, X.-H. Liu, and Q. Zhao, Phys.Rev. D92, 034022 (2015).
M. Mikhasenko, arXiv:1507.06552.

and others.

- Immediately after LHCb's Pc results (2019)

R. Chen, X. Liu, Z.-F. Sun, and S.-L. Zhu, arXiv:1903.11013 [hep-ph].

F. K. Guo, H. J. Jing, U.-G. Meissner, and S. Sakai, arXiv:1903.11503 [hep-ph].

J. He, arXiv:1903.11872 [hep-ph].

Hua-Xing Chen , Wei Chen, Shi-Lin Zhu, arXiv: 1903.11001 [hep-ph].

H. X. Huang, J. He, and J. L. Ping, arXiv: 1904.00221 [hep-ph].

C. J. Xiao, Y. Huang, Y. B. Dong, L. S. Geng, and D. Y. Chen, arXiv:1904.00872 [hep-ph].

M. Z. Liu, Y. W. Pan, F. Z. Peng, M. S. Sanchez, L. S. Geng, A. Hosaka, and M. P. Valderrama, , Phys. Rev. Lett. **122**, 242001 (2019)

and others.

- Some early studies

J. J. Wu, R. Molina, E. Oset and B. S. Zou, Phys. Rev. Lett. **105**, 232001 (2010) [arXiv:1007.0573 [nucl-th]].

J. J. Wu, R. Molina, E. Oset and B. S. Zou, Phys. Rev. C **84**, 015202 (2011) [arXiv:1011.2399 [nucl-th]].

J. J. Wu, T.-S. H. Lee and B. S. Zou, Phys. Rev. C **85**, 044002 (2012) [arXiv:1202.1036 [nucl-th]].

Z. C. Yang, Z. F. Sun, J. He, X. Liu and S. L. Zhu, Chin. Phys. C **36**, 6 (2012) [arXiv:1105.2901 [hep-ph]].

and others.

➢ Our work

1) Dynamic calculation in the limited space

H. X. Huang, C. R. Deng, J. L. Ping, and F. Wang, Eur. Phys. J. C. 76, 624 (2016), arXiv: 1510.04648.

- One bound state: $J^P = 1/2^-$ Nηc
- Resonance states? (Strong attraction between Σc/Σc* and D/ D*)

$J^P = 1/2^-$ ΣcD, ΣcD*, Σc*D*
$J^P = 3/2^-$ Σc∗D, ΣcD∗, Σc∗D∗, NJ/ψ
$J^P = 5/2^-$ Σc*D*

These states should couple to open channels to check whether they are resonance states or not.

2) Resonance states in the scattering process

H. X. Huang and J. L. Ping, Phys. Rev. D. 99, 014010 (2019) , arXiv: 1811.04260.

Six resonance states were found:

$J^P = 1/2^-$ ΣcD, ΣcD*, Σc*D*
$J^P = 3/2^-$ Σc∗D, ΣcD∗, Σc∗D*

1. Hidden-charm pentaquarks

Eur. Phys. J. C. 76, 624 (2016)

- The hidden charm pentaquark channels with I=1/2

Table 3 The channels involved in the calculation

$S=\frac{1}{2}$	$N\eta_c$	NJ/ψ	$\Lambda_c D$	$\Lambda_c D^*$	$\Sigma_c D$
	$\Sigma_c D^*$	$\Sigma_c^* D^*$			
$S=\frac{3}{2}$	NJ/ψ	$\Lambda_c D^*$	$\Sigma_c D^*$	$\Sigma_c^* D$	$\Sigma_c^* D^*$
$S=\frac{5}{2}$	$\Sigma_c^* D^*$				

✓ The state with the positive parity is unbound in present calculations.

- The effective potentials

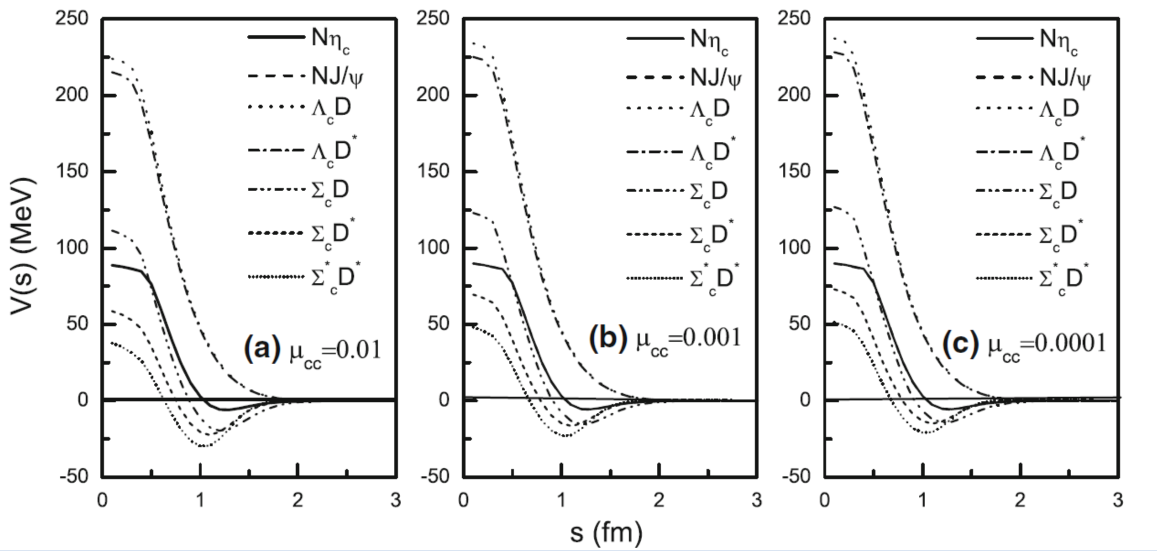

Fig. 1 The potentials of different channels for the $IJ^P=\frac{1}{2}\frac{1}{2}^-$ system

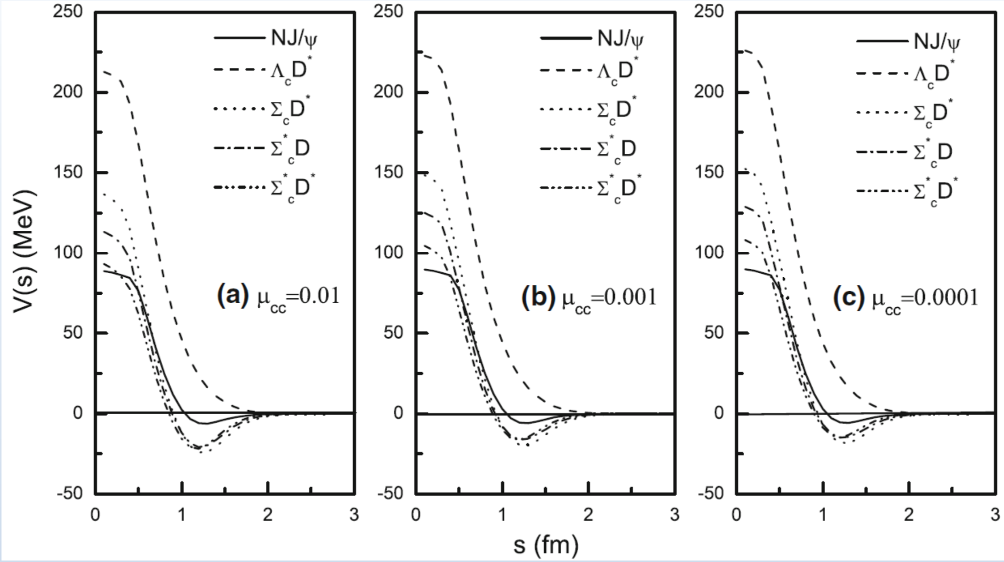

Fig. 2 The potentials of different channels for the $IJ^P = \frac{1}{2}\frac{3}{2}^-$ system

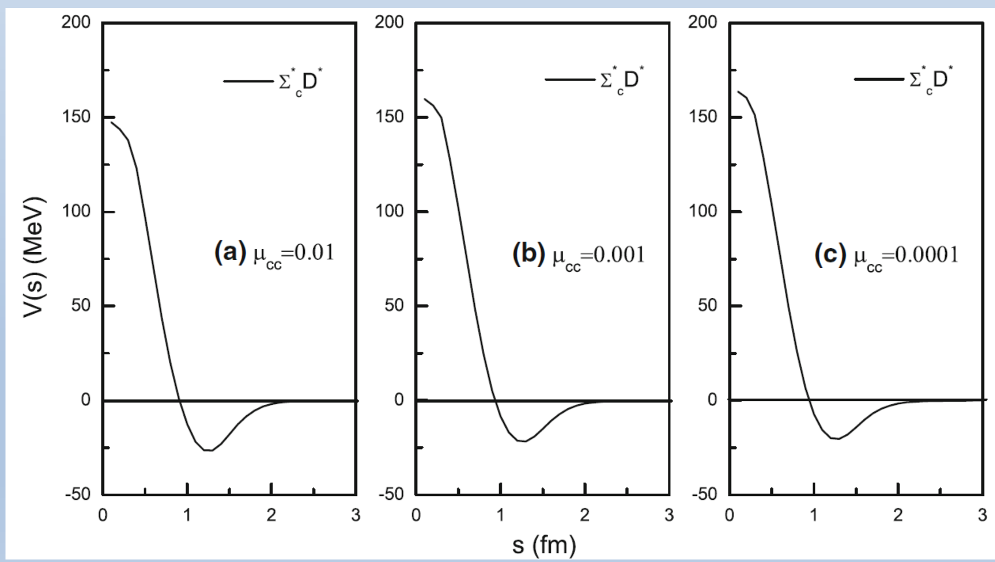

Fig. 3 The potential of a single channel for the $IJ^P = \frac{1}{2}\frac{5}{2}^-$ system

- ✓ The potentials are repulsive between *Λ*c and D/D*. So no bound states or resonances can be formed in these two channels *ΛcD and ΛcD**.
- ✓ Strong attractions between Σc/Σc* and D/D*.
- ✓ It is possible for Σc/Σc* and D/ D* to form bound states or resonance states.

- The single channel calculation

$J^P = \frac{1}{2}^-$				$J^P = \frac{3}{2}^-$			
μ_{cc}	0.01	0.001	0.0001	μ_{cc}	0.01	0.001	0.0001
$N\eta_c$	ub	ub	ub	NJ/ψ	ub	ub	ub
NJ/ψ	ub	ub	ub	$\Lambda_c D^*$	ub	ub	ub
$\Lambda_c D$	ub	ub	ub	$\Sigma_c D^*$	-16/4446	-11/4451	-10/4452
$\Lambda_c D^*$	ub	ub	ub	$\Sigma_c^* D$	-17/4367	-14/4370	-12/4372
$\Sigma_c D$	−19/4300	−15/4304	−13/4306	$\Sigma_c^* D^*$	−17/4510	−15/4512	−13/4514
$\Sigma_c D^*$	−21/4441	−19/4443	−18/4444	$J^P = \frac{5}{2}^-$			
$\Sigma_c^* D^*$	−24/4503	−23/4504	−21/4506	$\Sigma_c^* D^*$	−15/4512	−10/4517	−10/4517

$\neq$ **Pc(4450)**

Pc(4380)

Comparing with the LHCb's result in 2015

✓ The main component of the Pc(4380) maybe Σc*D with $J^P = 3/2^-$.

✓ The mass of the ΣcD* with $J^P = 3/2^-$ is close to the reported Pc(4450), but the opposite parity of this state to Pc(4380) may prevent one from making this assignment at that time.

- The channel-coupling calculation

Table 6 The masses (in MeV) of the hidden-charm molecular pentaquarks with all channels coupling and the percentages of each channel in the eigen-states

$J^P=\frac{1}{2}^-$				$J^P=\frac{3}{2}^-$				$J^P=\frac{5}{2}^-$			
μ_{cc}	0.01	0.001	0.0001	μ_{cc}	0.01	0.001	0.0001	μ_{cc}	0.01	0.001	0.0001
M_{cc}	3881	3883	3884	M_{cc}	3997	3998	3998	M_{cc}	4512	4517	4517
$N\eta_c$	41.7	49.7	35.2	NJ/ψ	80.8	71.0	62.1	$\Sigma_c^*D^*$	100.0	100.0	100.0
NJ/ψ	23.1	24.4	29.3	Λ_cD^*	8.7	11.9	15.9				
Λ_cD	14.6	11.7	14.5	Σ_cD^*	1.2	1.9	2.6				
Λ_cD^*	0.9	0.4	2.0	Σ_c^*D	3.5	5.8	7.3				
Σ_cD	0.1	4.8	6.0	$\Sigma_c^*D^*$	5.8	9.4	12.1				
Σ_cD^*	4.5	6.4	12.4								
$\Sigma_c^*D^*$	15.1	2.6	0.6								

- ✓ A bound state: $J^P = 1/2^-$ Nηc
- ✓ $J^P = 3/2^-$ NJ/ψ (*decay to open channels: D−wave Nηc*)
- ✓ $J^P = 5/2^-$ Σc*D* (*decay to open channels: some D−wave channels*)
- ✓ Where are these states?

$J^P = 1/2^-$ ΣcD, ΣcD*, Σc*D* *(decay to open channels: S-wave Nηc, NJ/ψ, ΛcD, ΛcD* and some D-wave channels)*

$J^P = 3/2^-$ Σc*D, ΣcD*, Σc*D* *(decay to open channels: S−wave NJ/ψ, ΛcD* and some D−wave channels)*

They maybe the resonance states.

To check whether they are resonance states or not, the study of scattering process of the corresponding open channels are needed !

- Resonance states in the scattering process

(1) $J^P = 1/2^-$

arXiv: 1811.04260, Phys. Rev. D. 99, 014010 (2019)

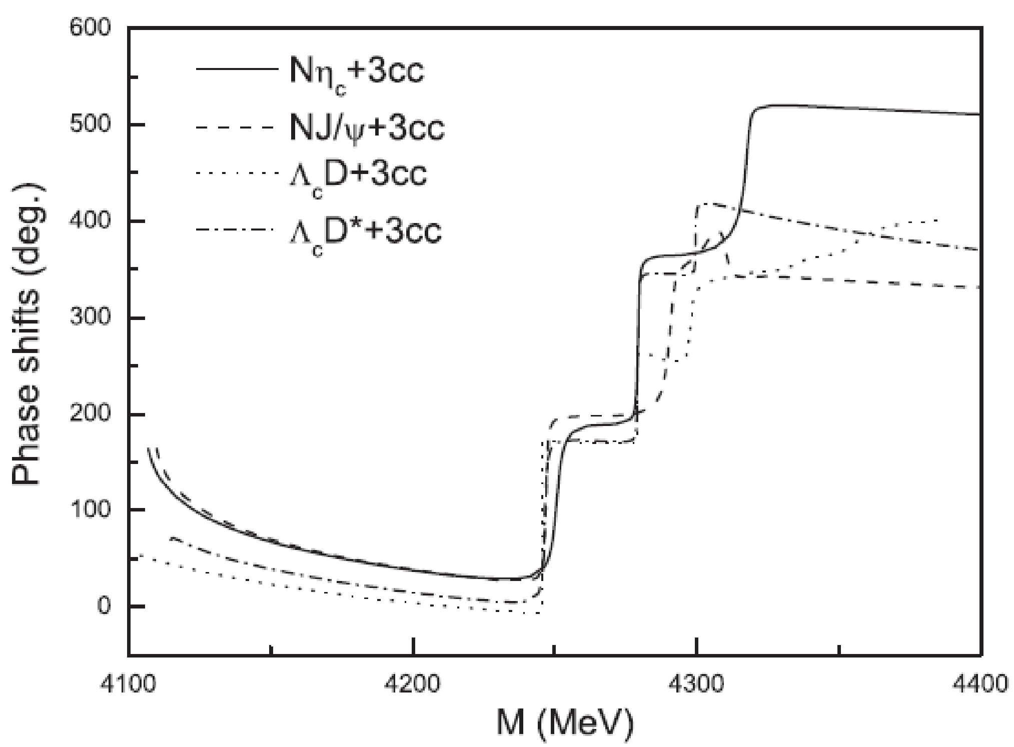

FIG. 2. The $N\eta_c$, NJ/ψ, $\Lambda_c D$, and $\Lambda_c D^*$ S-wave phase shifts with four-channel coupling for the $IJ^P = \frac{1}{2}\frac{1}{2}^-$ system.

- There are three resonance states: ΣcD, ΣcD*, and Σc*D* in the Nηc scattering phase shifts.
- In other scattering channels there are only two resonance states: ΣcD and ΣcD*.
- There is only a cusp around the threshold of the third state Σc*D*, because the channel coupling pushes the higher state above the threshold.

TABLE II. The masses and decay widths (in MeV) of the $IJ^P = \frac{1}{2}\frac{1}{2}^-$ resonance states in the $N\eta_c$, NJ/ψ, $\Lambda_c D$, and $\Lambda_c D^*$ S-wave scattering process.

	Two-channel coupling						Four-channel coupling					
	$\Sigma_c D$		$\Sigma_c D^*$		$\Sigma_c^* D^*$		$\Sigma_c D$		$\Sigma_c D^*$		$\Sigma_c^* D^*$	
	M'	Γ_i	M'	Γ_i	M'	Γ_i	M'	Γ_i	M'	Γ_i	M'	Γ_i
$N\eta_c$	4312.9	6.0	4451.7	1.1	4523.1	3.5	4311.3	4.5	4448.8	1.0	4525.8	4.0
NJ/ψ	4309.9	2.0	4461.6	4.0	4514.7	1.2	4307.9	1.2	4459.7	3.9	nr	$\cdots$
$\Lambda_c D$	4308.4	0.003	4452.6	1.0	4512.6	0.004	4306.7	0.02	4461.6	1.0	nr	$\cdots$
$\Lambda_c D^*$	4311.6	3.5	4452.5	1.0	4510.8	0.005	4307.7	1.4	4449.0	0.3	nr	$\cdots$
Γ_{total}		11.5		7.1		4.7		7.1		6.2		4.0

Pc(4312) **Pc(4457)**

(2) $J^P = 3/2^-$

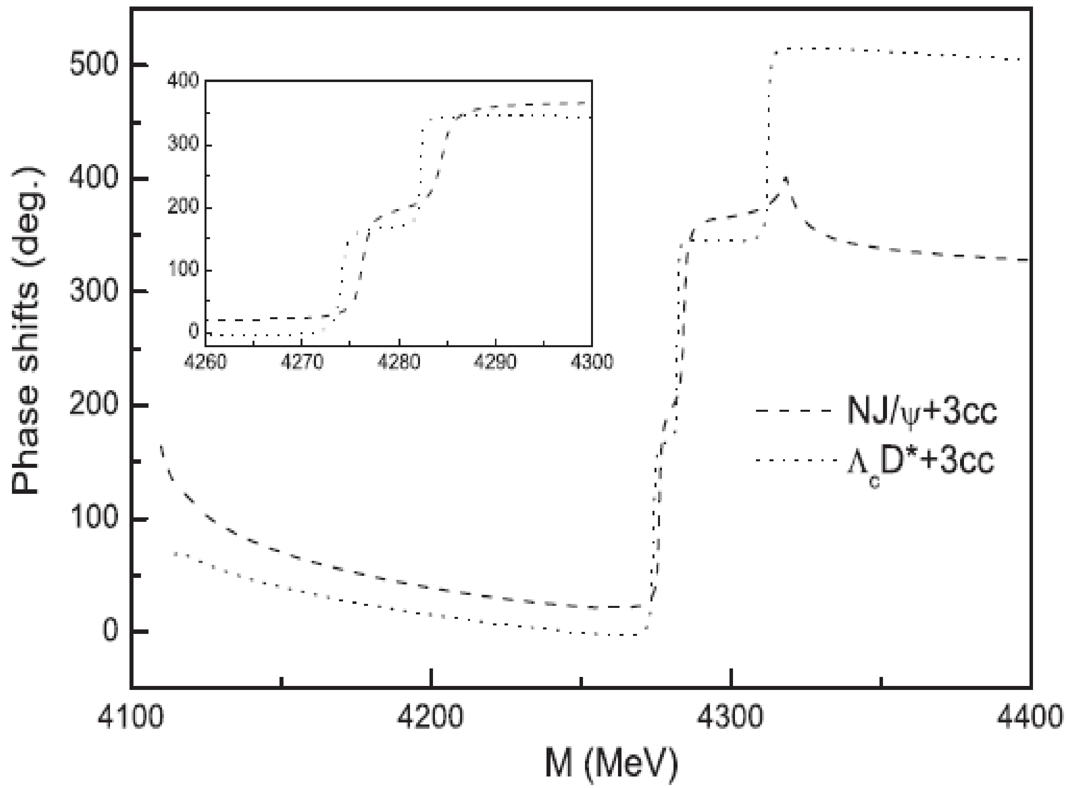

FIG. 4. The NJ/ψ and $\Lambda_c D^*$ S-wave phase shifts with four-channel coupling for the $IJ^P = \frac{1}{2}\frac{3}{2}^-$ system.

- There are two resonance states: ΣcD* and Σc*D in the NJ/ψ scattering phase shifts.
- There are three resonance states: ΣcD*, Σc*D and Σc*D* in the ΛcD* scattering phase shifts.

TABLE III. The masses and decay widths (in MeV) of the $IJ^P = \frac{1}{2}\frac{3}{2}^-$ resonance states in the NJ/ψ and $\Lambda_c D^*$ S-wave scattering process.

	Two-channel coupling					
	$\Sigma_c D^*$		$\Sigma_c^* D$		$\Sigma_c^* D^*$	
	M'	Γ_i	M'	Γ_i	M'	Γ_i
NJ/ψ	4453.8	1.7	4379.7	4.5	4526.4	2.5
$\Lambda_c D^*$	4452.7	0.8	4377.6	3.2	4522.7	1.8
Γ_{total}		2.5		7.7		4.3
	Four-channel coupling					
	$\Sigma_c D^*$		$\Sigma_c^* D$		$\Sigma_c^* D^*$	
	M'	Γ_i	M'	Γ_i	M'	Γ_i
NJ/ψ	4445.7	1.5	4376.4	1.5	nr	$\cdots$
$\Lambda_c D^*$	4444.0	0.3	4374.4	0.9	4523.0	1.0
Γ_{total}		$\boxed{1.8}$		? $\boxed{2.4}$		1.0

Pc(4440)

Pc(4380)

- Compare with the experiment

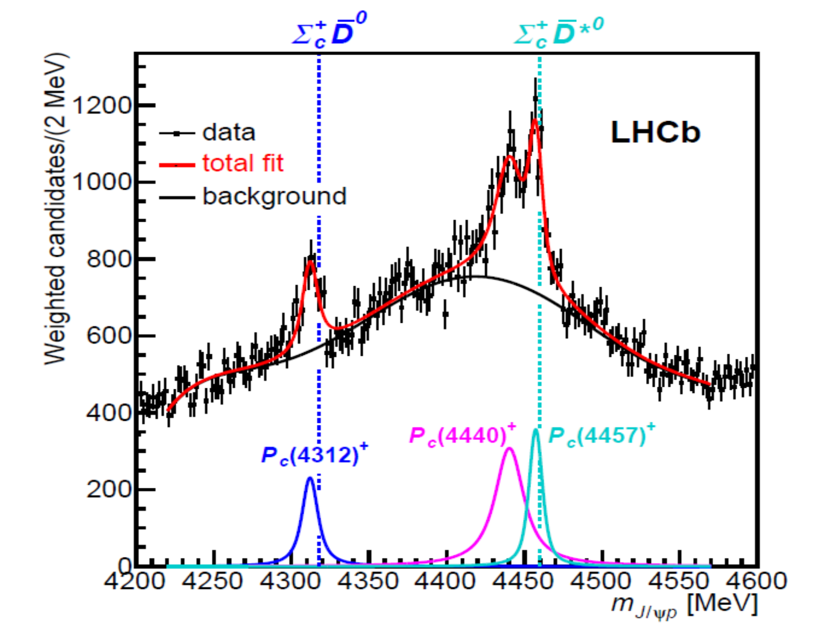

Figure 6: Fit to the $\cos\theta_{P_c}$-weighted $m_{J/\psi p}$ distribution with three BW amplitudes and a sixth-order polynomial background. This fit is used to determine the central values of the masses and widths of the P_c^+ states. The mass thresholds for the $\Sigma_c^+\bar{D}^0$ and $\Sigma_c^+\bar{D}^{*0}$ final states are superimposed.

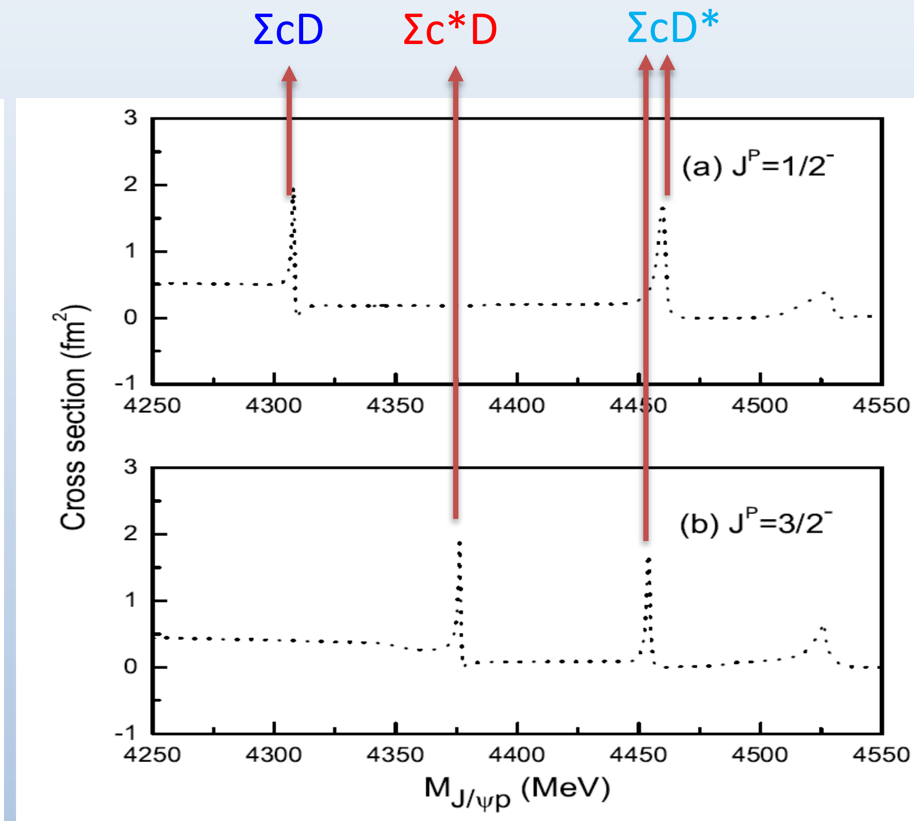

LHCb Collaboration,
Phys. Rev. Lett. 122 222001 (2019)

Phys. Rev. D. 99, 014010 (2019),
arXiv: 1904.00221

2. Hidden-bottom pentaquarks

(1) $J^P = 1/2^-$

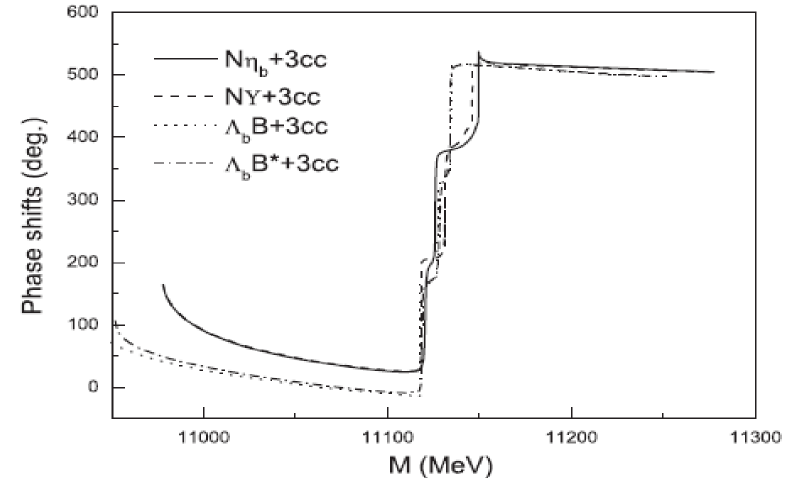

FIG. 6. The $N\eta_b$, $N\Upsilon$, $\Lambda_b B$ and $\Lambda_b B^*$ S-wave phase shifts with four-channel coupling for the $IJ^P = \frac{1}{2}\frac{1}{2}^-$ system.

TABLE IV. The masses and decay widths (in MeV) of the $IJ^P = \frac{1}{2}\frac{1}{2}^-$ resonance states in the $N\eta_b$, $N\Upsilon$, $\Lambda_b B$, and $\Lambda_b B^*$ S-wave scattering process.

	Two-channel coupling						Four-channel coupling					
	$\Sigma_b B$		$\Sigma_b B^*$		$\Sigma_b^* B^*$		$\Sigma_b B$		$\Sigma_b B^*$		$\Sigma_b^* B^*$	
	M'	Γ_i	M'	Γ_i	M'	Γ_i	M'	Γ_i	M'	Γ_i	M'	Γ_i
$N\eta_b$	11 083.3	4.0	11 123.9	1.4	11 154.5	4.7	11 079.8	1.2	11 120.6	0.4	11 156.9	2.0
$N\Upsilon$	11 080.4	1.4	11 135.4	6.6	11 146.2	2.0	11 077.5	0.1	11 125.8	0.8	11 153.5	3.0
$\Lambda_b B$	11 079.0	0.000 3	11 125.4	2.0	11 145.1	0.49	11 077.2	0.001	11 122.0	0.6	11 141.8	0.1
$\Lambda_b B^*$	11 082.2	2.6	11 126.2	2.3	11 142.7	0.22	11 078.3	0.3	11 123.0	1.2	11 141.5	0.4
Γ_{total}		7.0		12.3		7.4		$\boxed{1.6}$		$\boxed{3.0}$		$\boxed{5.5}$

(2) $J^P = 3/2^-$

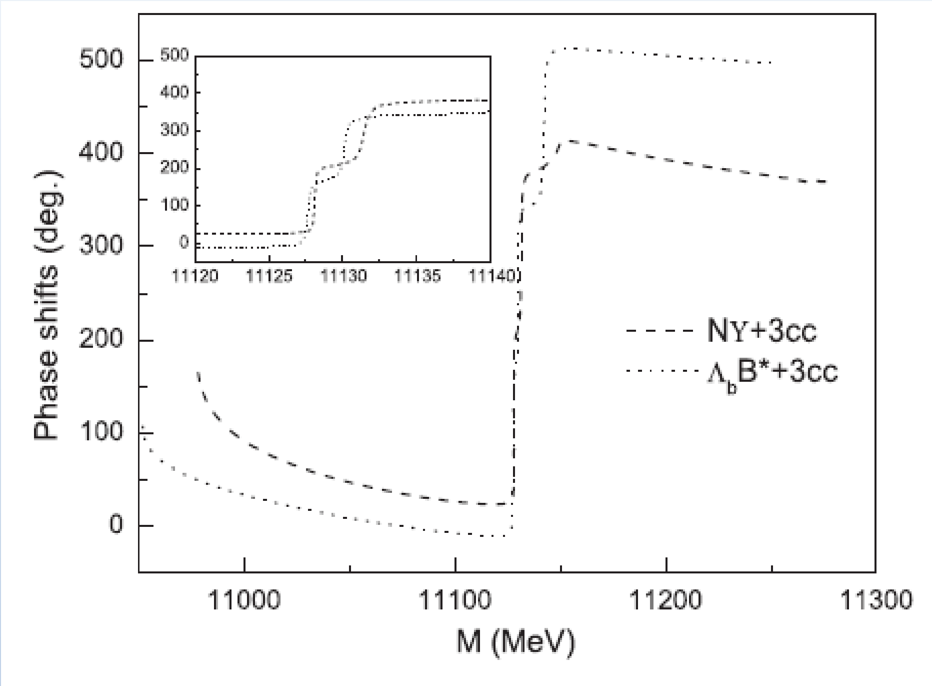

FIG. 8. The $N\Upsilon$ and $\Lambda_b B^*$ S-wave phase shifts with four-channel coupling for the $IJ^P = \frac{1}{2}\frac{3}{2}^-$ system.

TABLE V. The masses and decay widths (in MeV) of the $IJ^P = \frac{1}{2}\frac{3}{2}^-$ resonance states in the $N\Upsilon$ and $\Lambda_b B^*$ S-wave scattering process.

	Two-channel coupling					
	$\Sigma_b B^*$		$\Sigma_b^* B$		$\Sigma_b^* B^*$	
	M'	Γ_i	M'	Γ_i	M'	Γ_i
$N\Upsilon$	11 126.3	1.7	11 105.8	4.4	11 155.7	3.8
$\Lambda_b B^*$	11 125.5	0.9	11 103.5	2.6	11 152.0	2.7
Γ_{total}		2.6		7.0		6.5
	Four-channel coupling					
	$\Sigma_b B^*$		$\Sigma_b^* B$		$\Sigma_b^* B^*$	
	M'	Γ_i	M'	Γ_i	M'	Γ_i
$N\Upsilon$	11 122.7	0.2	11 103.6	0.8	nr	$\cdots$
$\Lambda_b B^*$	11 122.2	0.2	11 102.4	0.3	$\boxed{11\ 150.0}$	$\boxed{1.8}$
Γ_{total}		$\boxed{0.4}$		$\boxed{1.1}$		1.8

- The results are similar to the hidden-charm pentaquarks.
- Some narrow hidden-bottom pentaquark resonances above 11 GeV are found from corresponding scattering process.

3. Hidden-strange pentaquark Nϕ

- The Nϕ bound state was first studied by H. Gao .

PRC 63 (2001) 022201(R)

The QCD van der Waals attractive potential is strong enough to bind a ϕ meson onto a nucleon inside a nucleus to form a bound state.

- The feasibility of experimental search for the Nϕ bound state at Jefferson Lab was demonstrated by H. Gao .

PRC 75 (2007) 058201

- Measurement of coherent ϕ-meson photoproduction from the deuteron.

CLAS Collaboration, PRC 76 (2007) 052202(R)
PLB 680 (2009) 417-422, PLB 696 (2011) 338-342

- The Nϕ was a quasi-bound state in the extended chiral SU(3) quark model.

PRC 73 (2006) 025207

- Search for a hidden strange baryon-meson bound state from φ production in a nuclear medium.

PRC 95 (2017) 055202

- The hidden strange pentaquark channels

TABLE II. The coupling channels of each quantum number.

J^P	$^{2S+1}L_J$	Channels
$\frac{1}{2}^-$	$^2S_{\frac{1}{2}}$	$N\eta'$, $N\phi$, ΛK, ΛK^*, ΣK, ΣK^*, $\Sigma^* K^*$
	$^4D_{\frac{1}{2}}$	$N\phi$, ΛK^*, ΣK^*, $\Sigma^* K$, $\Sigma^* K^*$
$\frac{3}{2}^-$	$^2D_{\frac{3}{2}}$	$N\eta'$, $N\phi$, ΛK, ΛK^*, ΣK, ΣK^*, $\Sigma^* K^*$
	$^4S_{\frac{3}{2}}(^4D_{\frac{3}{2}})$	$N\phi$, ΛK^*, ΣK^*, $\Sigma^* K$, $\Sigma^* K^*$
$\frac{5}{2}^-$	$^2D_{\frac{5}{2}}$	$N\eta'$, $N\phi$, ΛK, ΛK^*, ΣK, ΣK^*, $\Sigma^* K^*$
	$^4D_{\frac{5}{2}}$	$N\phi$, ΛK^*, ΣK^*, $\Sigma^* K$, $\Sigma^* K^*$
$\frac{1}{2}^+$	$^2P_{\frac{1}{2}}$	$N\eta'$, $N\phi$, ΛK, ΛK^*, ΣK, ΣK^*, $\Sigma^* K^*$
	$^4P_{\frac{1}{2}}$	$N\phi$, ΛK^*, ΣK^*, $\Sigma^* K$, $\Sigma^* K^*$
$\frac{3}{2}^+$	$^2P_{\frac{3}{2}}$	$N\eta'$, $N\phi$, ΛK, ΛK^*, ΣK, ΣK^*, $\Sigma^* K^*$
	$^4P_{\frac{3}{2}}$	$N\phi$, ΛK^*, ΣK^*, $\Sigma^* K$, $\Sigma^* K^*$
$\frac{5}{2}^+$	$^4P_{\frac{5}{2}}$	$N\phi$, ΛK^*, ΣK^*, $\Sigma^* K$, $\Sigma^* K^*$

✓ The states of P and D wave are unbound in present calculations.

- The effective potentials

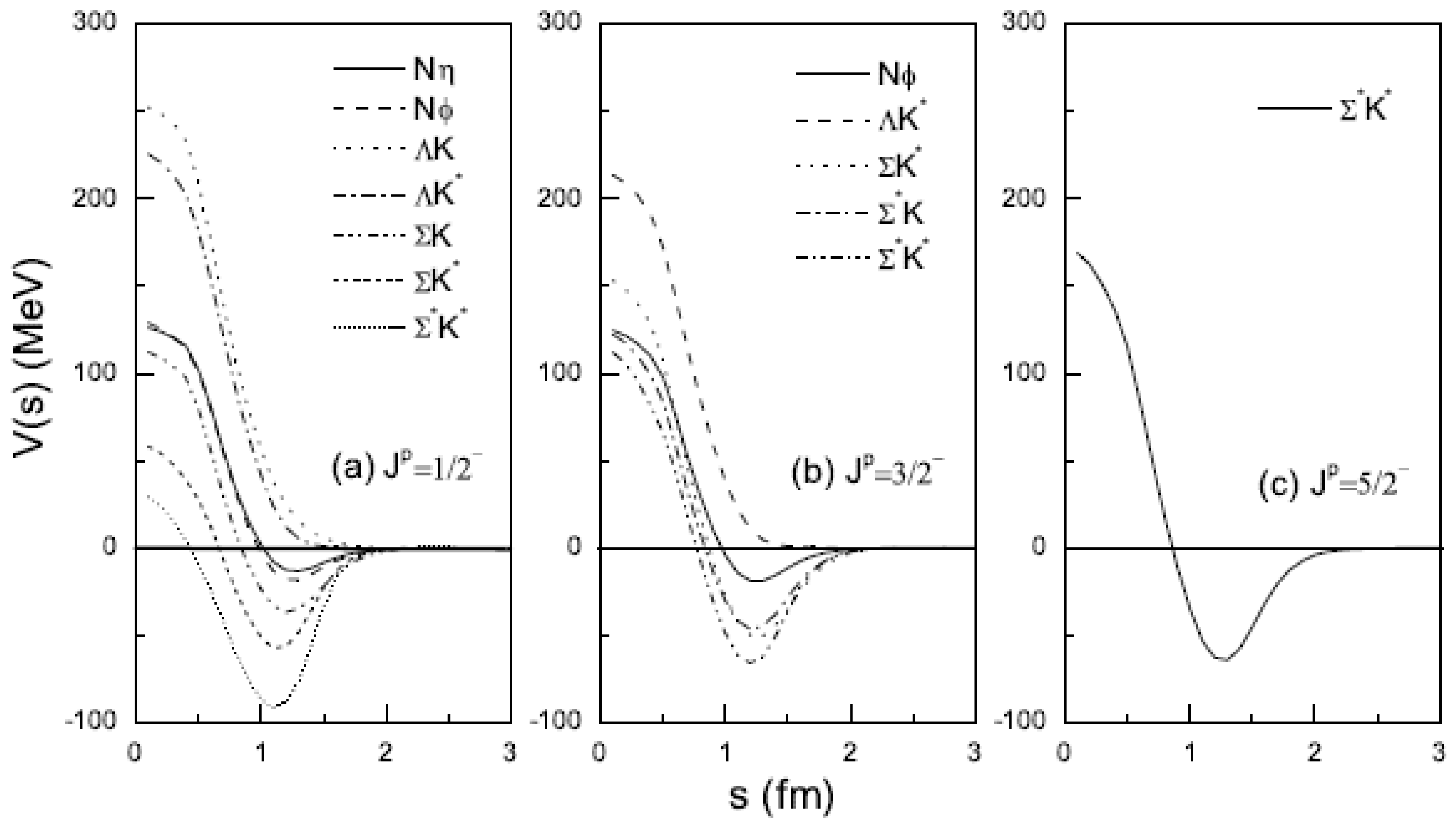

FIG. 1: The potentials of different channels for the $I = \frac{1}{2}$, $J^P = \frac{1}{2}^-, \frac{3}{2}^-, \frac{5}{2}^-$ systems.

- # The bound state calculation

TABLE III. The binding energy and the total energy of each individual channel and all coupled channels for the two S-wave bound states with the quantum numbers $J^P = \frac{1}{2}^-$ and $\frac{3}{2}^-$. The values are provided in units of MeV, and "ub" represents unbound.

Channel	$J^P = \frac{1}{2}^-$			$J^P = \frac{3}{2}^-$		
	QDCSM1	QDCSM2	QDCSM3	QDCSM1	QDCSM2	QDCSM3
$N\eta'$	ub	ub	ub	–	–	–
$N\phi$	ub	ub	ub	ub	ub	ub
ΛK	ub	ub	ub	–	–	–
ΛK^*	ub	ub	ub	ub	ub	ub
ΣK	−6.7/1681.3	−26.8/1661.2	−4.9/1683.1	–	–	–
ΣK^*	−8.9/2076.1	−30.6/2054.4	−22.4/2062.2	−21.6/2063.4	−21.1/2063.9	−21.2/2063.8
$\Sigma^* K$	–	–	–	−10.4/1869.6	−15.5/1864.5	−11.1/1868.9
$\Sigma^* K^*$	−17.3/2259.7	−87.0/2190.0	−73.9/2203.1	−11.3/2265.7	−18.4/2258.6	−27.2/2249.8
Coupled	−16.0/1881.0	−20.0/1877.0	−24.3/1872.7	−10.1/1948.9	−7.7/1951.3	−1.6/1957.4

- ✓ Nη’ is a bound state by channel-coupling calculation.
- ✓ Nϕ may be a resonance state.

- Resonance states in the scattering process

(1) Nϕ

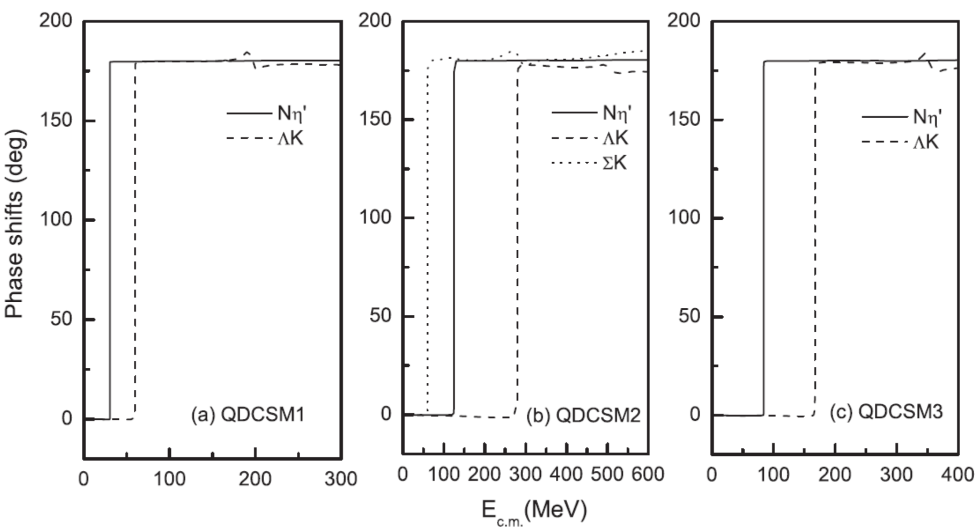

FIG. 1. The phase shifts of different scattering channels for the $J^P = \frac{3}{2}^-$ systems.

TABLE IV. The $N_{s\bar{s}}$ bound state mass calculated from the ${}^2D_{\frac{3}{2}}$ scattering channels. The values are provided in units of MeV.

Scattering channel	QDCSM1	QDCSM2	QDCSM3
$N\eta'$	1947.998	1949.485	1955.988
ΛK	1947.975	1949.480	1955.910
ΣK	–	1949.597	–

TABLE V. The decay widths and branch ratios of each decay channel of $N_{s\bar{s}}$ bound state.

Decay channel	QDCSM1		QDCSM2		QDCSM3	
	Γ_i(MeV)	Γ_i/Γ(%)	Γ_i(MeV)	Γ_i/Γ(%)	Γ_i(MeV)	Γ_i/Γ(%)
$N\eta'$	0.002	0.1	0.022	0.5	0.009	0.2
ΛK	0.011	0.3	0.120	2.9	0.055	1.2
ΣK	–	0.0	0.060	1.5	–	0.0
ϕ decays	3.619	99.6	3.892	95.1	4.616	98.6

(2) Pc-like resonances

PRD 97 (2018) 094019

TABLE IV. The resonance mass and decay width (in MeV) of the molecular pentaquarks with $J^P = \frac{1}{2}^-$.

	ΣK		ΣK^*		$\Sigma^* K^*$	
S wave	M_r	Γ_i	M_r	Γ_i	M_r	Γ_i
$N\eta'$	...	...	2079.4	1.1	2246.8	20.0
$N\phi$	...	...	2080.0	3.6	2237.0	30.0
ΛK	1668.0	1.3	2083.4	1.0	2261.5	20.0
ΛK^*	...	...	2056.6	0.2	2219.0	58.0
ΣK	...	...	2071.6	4.6	2252.3	6.0
ΣK^*	...	...	...	...	2253.9	16.0
D wave						
$N\phi$	...	...	2076.3	0.3	2254.4	0.006
ΛK^*	...	...	2076.3	0.4	2253.6	0.6
ΣK^*	...	...	...	...	2254.0	0.06
$\Sigma^* K$	...	...	2076.8	0.01	2253.3	0.8

TABLE V. The resonance mass and decay width (in MeV) of the molecular pentaquarks with $J^P = \frac{3}{2}^-$.

	ΣK^*		$\Sigma^* K$		$\Sigma^* K^*$	
S wave	M_r	Γ_i	M_r	Γ_i	M_r	Γ_i
$N\phi$	2060.6	10.4	...	...	2270.5	0.03
ΛK^*	2046.1	15.0	...	...	2256.5	2.0
ΣK^*	...	...	...	...	2270.6	0.1
$\Sigma^* K$	2054.1	2.3	...	...	2263.6	3.7
D wave						
$N\eta'$	2061.4	0.001	1875.7	0.0004	2269.2	0.01
$N\phi$	2061.0	0.2	...	...	2269.3	0.01
ΛK	2060.6	0.9	1871.6	0.08	2269.2	0.02
ΛK^*	2059.1	0.3	...	...	2269.1	0.05
ΣK	2060.3	0.9	1871.6	0.05	2269.2	0.02
ΣK^*	...	...	...	...	2269.2	0.003

N*(2100) **N*(1875)**

VI. Summary

➢ Dibaryons

1. Nonstrange dibaryon

A compact six quark state $\boldsymbol{IJ^P} = 03^+$ d*

2. Strange dibaryon

A narrow resonance $\boldsymbol{IJ^P} = \frac{1}{2}2^+$ NΩ

3. Dibaryon with heavy quarks:

H-like dibaryon states: $\Lambda_c\Lambda_c$ and $\Lambda_b\Lambda_b$

NΩ-like dibaryons states: $N\Omega_{ccc}$ and $N\Omega_{bbb}$

Pentaquarks

1. Hidden-strange pentaquark

1 bound state: $J^P = 1/2^-$ Nη'

8 resonance states: $J^P = 1/2^-$ ΣK, ΣK^*, $\Sigma^* K^*$

$J^P = 3/2^-$ $\Sigma^* K$ ($N^*(1875)$), ΣK^*($N^*(2100)$), $\Sigma^* K^*$, Nϕ

$J^P = 5/2^-$ $\Sigma^* K^*$

2. Hidden-charm pentaquark

1 bound state: $J^P = 1/2^-$ Nη_c

8 resonance states: $J^P = 1/2^-$ $\Sigma_c D$ ($P_c(4312)$), $\Sigma_c D^*$ ($P_c(4457)$), $\Sigma_c^* D^*$

$J^P = 3/2^-$ $\Sigma_c^* D$ ($P_c(4380)$), $\Sigma_c D^*$ ($P_c(4440)$), $\Sigma_c^* D^*$, NJ/ψ

$J^P = 5/2^-$ $\Sigma_c^* D^*$

3. Hidden-bottom pentaquark

1 bound state: $J^P = 1/2^-$ Nη_b

8 resonance states: $J^P = 1/2^-$ $\Sigma_b B$, $\Sigma_b B^*$, $\Sigma_b^* B^*$

$J^P = 3/2^-$ $\Sigma_b^* B$, $\Sigma_b B^*$, $\Sigma_b^* B^*$, NΥ

$J^P = 5/2^-$ $\Sigma_b^* B^*$

Thanks for your attention!